Amino Acid Signatures in the Normal Cat Retina

Robert E. Marc,[1] Ralph F. Murry,[1] Steven K. Fisher,[2] Kenneth A. Linberg,[2] Geoffrey P. Lewis,[2] and Michael Kalloniatis[3]

Purpose. To establish a nomogram of amino acid signatures in normal neurons, glia, and retinal pigment epithelium (RPE) of the cat retina, guided by the premise that micromolecular signatures reflect cellular identity and metabolic integrity. The long-range objective was to provide techniques to detect subtle aberrations in cellular metabolism engendered by model interventions such as focal retinal detachment.

Methods. High-performance immunochemical mapping, image registration, and quantitative pattern recognition were combined to analyze the amino acid contents of virtually all cell types in serial 200-nm sections of normal cat retina.

Results. The cellular cohorts of the cat retina formed 14 separable biochemical theme classes. The photoreceptor → bipolar cell → ganglion cell pathway was composed of six classes, each possessing a characteristic glutamate signature. Amacrine cells could be grouped into two glycine- and three γ-aminobutyric acid (GABA)-dominated populations. Horizontal cells possessed a distinctive GABA-rich signature completely separate from that of amacrine cells. A stable taurine-glutamine signature defined Müller cells, and a broad-spectrum aspartate-glutamate-taurine-glutamine signature was present in the normal RPE.

Conclusions. In this study, basic micromolecular signatures were established for cat retina, and multiple metabolic subtypes were identified for each neurochemical class. It was shown that virtually all neuronal space can be accounted for by cells bearing characteristic glutamate, GABA, or glycine signatures. The resultant signature matrix constitutes a nomogram for assessing cellular responses to experimental challenges in disease models. (*Invest Ophthalmol Vis Sci.* 1998;39: 1685-1693)

The cat retina contains at least 59 types of retinal neurons[1] and two classes of macroglia of which the Müller cell is the dominant form.[2,3] In principle, every cell type possesses a distinctive molecular signature composed of "macromolecular" and "micromolecular" constituents. Micromolecular signatures reflect mixtures of low-molecular-weight metabolites characteristic of various cell types, and amino acids are a subset thereof. Amino acids are detectable by IgG probes with subcellular resolution and species-independent fidelity. In practice, only partial micromolecular signatures can be accessed, but they have proved to be powerful discriminanda for cell types and basal state.[4,5] We sought to establish a nomogram of amino acid signatures for feline retina (a prime model of mammalian retinal circuitry[6] and in experimental ophthalmology[7-9]) against which alterations in cellular status associated with environmental challenges could be assessed. This objective is plausible, because acute[10] and degenerative[11] insults evoke global alterations in central nervous system amino acid profiles.

Extracting quantitative signatures from cells requires detecting micromolecular contents with subcellular precision, correlating contents across all cells, and grouping cells into statistically separable sets with pattern-recognition algorithms. Such analyses parse more than 99% of cellular space in central retina of cynomolgus macaques into 16 unique glutamate-, γ-aminobutyric acid (GABA)-, or glycine-dominated neuronal classes and taurine-rich glia.[5] In this analysis, we showed that 14 distinct cell classes could be defined in the cat retina based on differential patterning of alanine, GABA, aspartate, glutamate, glutamine, glycine, and taurine signals. This differentiation included signatures of Müller cells and the retinal pigment epithelium (RPE). The taurine-glutamine signature of Müller cells is emerging as a constant across vertebrate phylogeny and is shared by fishes,[4] birds,[12] primates,[5] and 20 other vertebrate species (Marc RE, unpublished data, 1993-1998). The metabolic signatures of glia and the RPE are probably key indexes of regional retinal status: They are the portals through which most carbon skeletons central to neuronal metabolism must pass. Further, cat neuronal signatures show strong resemblances to those of primates and even disparate taxa such as cyprinids. This supports the hypothesis that different neuronal classes possess distinctive micromolecular profiles tuned to their neurochemical and functional roles. More important, however, the signatures of neurons, glia, and the RPE probably

From the [1]John Moran Eye Center, University of Utah, Salt Lake City; [2]Neuroscience Research Institute, University of California Santa Barbara; [3]Department of Optometry and Vision Sciences, University of Melbourne, Parkville, Victoria, Australia.

Supported in part by grants from the National Institutes of Health, Bethesda, Maryland: EY02576 (REM), National Research Service Award EY06651 (RFM), and EY00888 (SKF); a Jules and Doris Stein Professorship from the Research to Prevent Blindness, New York, New York (REM); grant from the Australian National Health and Medical Research Council: 940087 (MK), and the Australian Retinitis Pigmentosa Association Grant, Brisbane, Australia (MK).

Submitted for publication December 15, 1997; revised March 3, 1998; accepted April 14, 1998.

Proprietary interest category: P (REM).

Reprint requests: Robert E. Marc, John Moran Eye Center, University of Utah Health Sciences Center, 50 North Medical Drive, Salt Lake City, UT 84132.

connote their metabolic integrity, and amino acid profiles may serve as sensitive measures of normal and pathologic responses to biologic challenges.

METHODS

Tissue Preparation and Immunocytochemistry

All animal care was in accordance with institutional animal care and use guidelines and the ARVO Statement for the Use of Animals in Ophthalmic and Vision Research. Eyes were enucleated from adult cats euthanatized by pentobarbital overdose. Open eyecups immersion-fixed in 1% paraformaldehyde-1% glutaraldehyde in 0.086 M phosphate buffer (pH 7.4) were processed for electron microscopic-grade embedding in resin (Araldite 6005; Polysciences, Warrington, PA). Tissue was postfixed 1 hour in 2% buffered osmium. Serial 200-nm sections were cut onto 12-well slides, etched 30 minutes with saturated sodium methoxide, deosmicated for 10 minutes with 1% aqueous sodium metaperiodate, and probed with IgG targeting glutaraldehyde-conjugate haptens at the following serum dilutions: alanine (A), 1:5000; γ-aminobutyric acid (γ), 1:32000; aspartate (D), 1:2000; glutamate (E), 1:64000; glycine (G), 1:2000; glutamine (Q), 1:16000; and taurine (τ), 1:64000. For brevity, we refer to amino acids with the conventional single-letter code for the protein amino acids augmented for the nonprotein amino acids.[4] Binary signal patterns are referred to as positive and negative: for example, $GABA^+ \equiv \gamma^+$, $GABA^- \equiv \gamma^-$. All IgG were produced by the laboratory of REM or obtained from Signature Immunologics (Salt Lake City, UT). Primary IgG signals were detected with goat anti-rabbit IgG coated with 1-nm gold particles and visualized by silver intensification. These methods are detailed in Marc et al.[4,13] and Kalloniatis and Fletcher.[5] The data presented in this study were derived from three cats. No significant differences were documented across subjects.

Image Calibration, Signal Interpretation, and Image Registration

Light microscopic images of immunoreactivity were captured under constant-flux 550-nm (10-nm bandpass) light using fixed camera gain and gamma, yielding a log-linear pixel value scale over the range of usable irradiance and stored as 512-pixel × 480-line image frames. Digital images of immunoreactivity represent an estimate of intracellular concentration ranging from a lower limit of 0.05 mM to more than 10 mM.[13] Images from single sections were montaged and those from serial sections aligned to 250 nm or less root mean square error by conventional registration algorithms (PCI Remote Sensing, Richmond Hill, Ontario, Canada) using common anatomic landmarks as control points. Low-pass filtering was performed to suppress intracellular variations arising from intracellular inclusions. All images were inverted using a logical NOT operation so that increasing immunoreactivity scaled with increasing pixel value. Details of these methods are available in Marc et al.[4]

Image Visualization, Pattern Recognition, and Statistical Analysis

Image data were explored as aligned serial monochrome images, red-green-blue (rgb)-mapped images, and *N*-dimensional data sets resolved into statistically separable theme classes by pattern recognition.[4] Common points on registered images represent arrays of micromolecular signals linked to a specific structure in anatomic space. Monochrome exploration allows rapid discovery of simple correlations for nearly binary signals, for example, γ^+ versus γ^- cells. However, the numbers or types of cells cannot be easily or accurately determined by visual comparison of monochrome images. More comprehensive correlations among amino acid contents are achieved by assigning each amino acid signal to one color channel of a video monitor:amino acid → rgb mapping. Basic rgb mapping quickly reveals populations of cells dominated by characteristic complex signatures and also exposes those not captured as a class by a given set of signals. In the end, rgb mapping must be augmented with classic pattern-recognition methods to explore the *N*-dimensional amino acid data and extract statistically separable and significant cell classes. All theme classes described herein were defined by *k*-means clustering. To characterize outcomes by theme class, (described later) a bold, uppercase letter notation was used for the dominant presumed functional molecules of a theme class and ordinal notation for separable subsets (e.g., glutamate dominated classes ≡ **E1**, **E2**, and so on). Theme classes are statistical entities based on common sets of signal values and intervalue correlations, not anatomic features. Signature matrices were constructed for all cell classes as arrays of univariate probability histograms, fast-Fourier transform-filtered to a concentration resolution of 0.125 log units across a 2-log-unit range. All amino acid concentrations were plotted on an absolute scale. It is important to realize that there is no formal basis for expecting different cell classes to show statistically significant or separable groupings, and thus a failure to parse a group means little. However, a clear distinction between significant classes and separable classes is important. "Significant" classes are those whose univariate or multivariate distributions of signals clearly cannot be derived from the same population, although they may overlap greatly. Conversely, "separable" classes are those whose *N*-means and *N*-covariances in the entire data set are such that a member of that class would be successfully assigned to its proper group with less than 1% error. Separable classes are significant classes; the converse is not always true. The separability of theme classes is reported as transformed divergence (D^T), a statistic for estimating the degree of pairwise theme class segregation.[15] The standard cutoff for significance is D^T 1.9 or more, corresponding to a probability of error $P_e < 0.01$ for populations with equal a priori probability density functions. All theme classes reported were separable with D^T 1.9 or more.

RESULTS

The normal cat retina possesses four major types of micromolecular signatures, in accord with results described for a wide range of vertebrates.[4,5] Figure 1 summarizes these data as 2 of 35 possible unique amino acid triplet → rgb mappings from serial 200-nm vertical sections probed as the ADEGQτγ series. The top panel displays a γGE → rgb map, demonstrating three basic neuronal groupings: (1) dark blue-cyan photoreceptor, bipolar, and ganglion cells representing glutamate-rich class E neurons; (2) magenta-red amacrine and horizontal cells representing GABA-rich class Γ neurons; (3) green amacrine cells representing glycine-rich class **G** neurons. There is a significant amount of black, unclassified space in this image, and the γGE

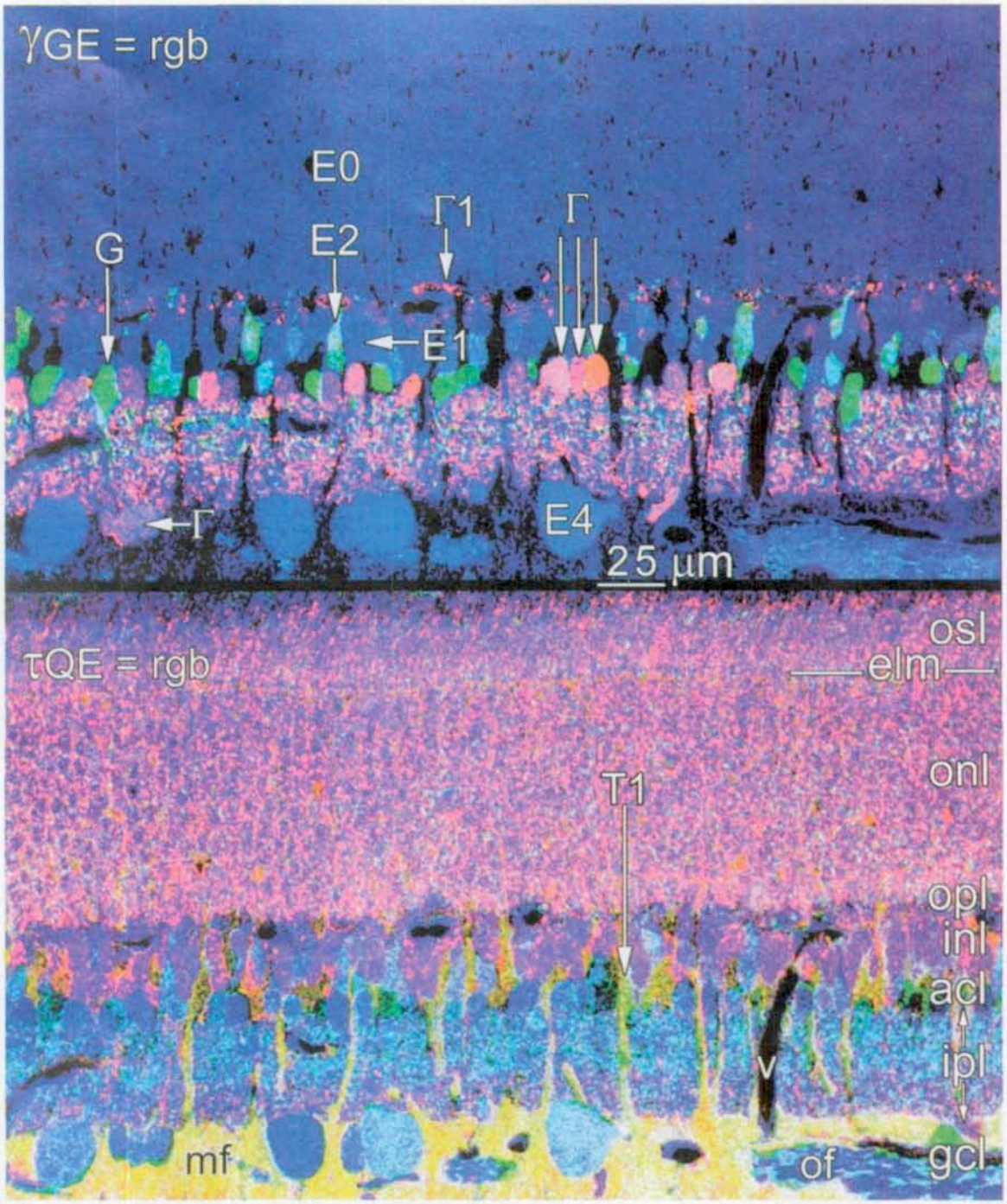

FIGURE 1. Amino acid → red-green-blue (rgb) mappings from registered serial 200-nm sections of midperipheral, superior retina of the normal cat. *Top*: γ-aminobutyric acid-glycine-glutamate (γGE) → rgb; *Bottom*: taurine-glutamine-glutamate (τQE) → rgb. Photoreceptors show a type **E0** signature, certain bipolar cells possess either **E1** or **E2** signatures, and most ganglion cells possess a type **E4** signature. Glycine-rich signatures are present in the amacrine cell layer, and γ-aminobutyric acid (GABA)-rich (Γ) signatures were present in the amacrine and ganglion cell layers. γ-Aminobutyric acid-rich horizontal cells display a Γ1 signature distinct from other presumed GABAergic neurons. However, γGE → rgb mapping leaves a significant amount of retinal space blank. Switching to a τQE → rgb mapping (*bottom*) shows that virtually all that space is occupied by a single distinctive **T1** signature belonging to Müller cells. The remaining unmapped space corresponds to the lumens of blood vessels (v). acl, amacrine cell layer; elm, external limiting membrane; gcl, ganglion cell layer; inl, inner nuclear layer; ipl, inner plexiform layer; mf, Müller cell foot pieces; of, optic fiber bundle; onl, outer nuclear layer; opl, outer plexiform layer; osl, outer segment layer. Size scale applies to both panels.

set clearly accounts for but a portion of all cell types. Because both panels of Figure 1 are in register and represent the same cellular elements, we may remap the image as a τQE → rgb set to show different micromolecular patterns. The τQE mapping showed that most of the black vacancies in the upper panel were comprised of Müller cell somas, processes, and end feet

visualized as orange-to-yellow signals representing the high levels of mixed taurine (red) and glutamine (green), with no significant glutamate content. All remaining unclassified areas were the lumens of blood vessels. These data imply that essentially all key neuronal and glial elements in the cat retina fell into one of these four basic classes. Careful comparisons of τQE and γGE mappings shows that the patterns of signals across cell types involved more than four simple groupings. Various γ^+ amacrine cells possessed a range of spectral signatures, and horizontal cell γ signals were weak compared with amacrine cell γ signals. Thus, the Γ group cannot be viewed as homogeneous. Similarly, not all bipolar cells possessed the same kind of $\mathbf{E}^+$ signature, and ganglion cells were different from photoreceptors and bipolar cells, although it is thought that all photoreceptors, all bipolar cells, and most ganglion cells are functionally glutamatergic.[13] τQE mapping showed that ganglion cells were distinguished from all other putative glutamatergic neurons by elevated glutamine and diminished taurine signals, a property shared by ganglion cells in primates,[5] birds,[12] and fishes.[4]

Different rgb signatures arise from different signal mixtures across cell populations, but rgb mappings cannot resolve the quantitative bases of diverse signal patterns. Proper analysis of signatures requires sampling signals from large numbers of neurons simultaneously. Oblique retinal sections allow easy discrimination of layers and enhance sampling efficiency. Figure 2 displays a small portion of a high-resolution database in which every channel is a mosaic of 15 to 20 individual tiles (each tile captured at a resolution of 300 nm/pixel) and eight channels mutually registered into the ADEGQτγ series, plus a toluidine blue channel. The top panel displays the γ signal in the cat retina, including the dendrites and somas of horizontal cells; somas of conventional and displaced amacrine cells in the inner nuclear layer and ganglion cell layers, respectively; and the essentially uniform distribution of γ^+ amacrine cell processes throughout the inner plexiform layer. All seven amino acid signals in the same patch of the inner nuclear layer are displayed in small fields beneath the top panel. In particular, it is easy to visualize how a characteristic signature can be derived for horizontal cells and that γ^+ and G^+ amacrine cells form largely exclusive sets in cat. However, roughly 8% to 12% of all γ^+ amacrine cells are strongly γ^+ and moderately G^+, thus forming a distinct **ΓG** class of amacrine cells similar to that found in primate[5] and salamander[16] retinas, described in cat by Kalloniatis and Tomisch.[17]

The metabolite signals ADQτ generally did not strongly identify any single cell class but showed variations across classes that contributed to multichannel discrimination of cell types. Müller cells possessed a strong τQ-dominated signature (Fig. 1), rendering them distinct from all other cellular classes. Normal Müller cells had no notable aspartate, glutamate, GABA, or glycine signals, despite their ability to transport GABA and glutamate effectively. The normal RPE also possessed distinctive aspartate, glutamate, glutamine, and taurine elevations with no significant GABA or glycine signals (Fig. 3).

All these data can be summarized quantitatively using multichannel *k*-means clustering. Each spatial coordinate in a multichannel image indexes a list of amino acid values from which statistically separable biochemical groups can be abstracted, each with a multichannel signature. The univariate histogram matrix (Fig. 4) is a simple means of displaying some signature features associated with different neuronal, glial, and epithelial classes in the cat retina. Figure 4 is the univariate histogram matrix for one cat. These patterns were stable across all three cats that were analyzed by *k*-means clustering. Each cat displayed 14 theme classes. Thus, any differences in class means and variances across cats were insufficient to alter the number or type of theme classes. Individual amino acid labeling patterns were analyzed in more than 20 cat samples with no deviations noted. Individual histogram values may have shifted as many as 0.3 log units, but no cat differed significantly from the population mean for a given value ($P > 0.25$). There were six glutamate-rich type **E**, two glycine-rich type **G**, four GABA-rich type Γ, and two taurine-containing type **T** classes, which together subsumed essentially all retinal cell types but vascular cells, astrocytes in the ganglion cell layer (not shown), and other cell types not easily sampled in our format (e.g., microglia).[18] Type **E** cells included rods and cones (**E0**), most bipolar cells (**E1**), glycine-rich bipolar cells (**E2**), GABA-containing bipolar cells (**E3**), most ganglion cells (**E4**), and a taurine-rich subset of ganglion cells (**E5**). These micromolecular types were differentiated solely by the statistical properties of their signatures, not their morphologies. The clear correspondence between micromolecular and morphologic sets, however, is robust evidence that different signatures represented metabolic tunings specific to their different functional roles. Type **G1** and **G2** glycine-rich amacrine cells were primarily distinguished by the absence of a strong taurine signal in one set (**G2**), which corresponded to the absence of a taurine signal in a set of glycine-rich **E2** bipolar cells. We suspect that **E2** and **G2** cells are coupled by gap junctions (see Discussion section). Similar to the primate and goldfish retinas, cat **Γ1** horizontal cells displayed a γ signal that was substantially weaker than that in amacrine cells. γ^+ amacrine cells were divisible into types **Γ2** and **Γ3**, based in part on differential low-level glycine and taurine contents. Whether these represent functional divisions remains to be seen.

Müller cells displayed a **T1** signature characteristically free of any primary neurotransmitter signals but dominated by glutamine and taurine. This simple and direct signature served as a key index of Müller cell status, as will be discussed later. Finally, the RPE had a complex **T2** signature with elevated taurine and glutamine levels, similar to Müller and many other

FIGURE 2. Mosaicked and registered oblique 200-nm sections probed for various amino acids. *Top*: a segment of a large mosaic of high-resolution tiles probed for γ signals, centered on the inner nuclear layer and including sublayers enriched in horizontal (h), bipolar (b), and amacrine cells (a). Large gaps that seem to be scratches or artifacts are γ^- blood vessels (V →). *Center*: the signals of the neurotransmitter amino acids, γ, γ-aminobutyric acid; G, glycine; and E, glutamate, which represent the rectangle on the *top* panel. *Bottom*: the remaining amino acid signals, A, alanine; D, aspartate; Q, glutamine; and τ, taurine, represent the same region with a right border indicated by the *vertical line* in the rectangle. A single γ^+ horizontal cell, a **ΓG** amacrine cell, and a blood vessel (bv) are indicated in various center and bottom panels. (G) represents glycine signals, and all γ^+ amacrine cell somas are indicated by *vertical arrows*. The scale in γ applies to all *center* and *bottom* panels.

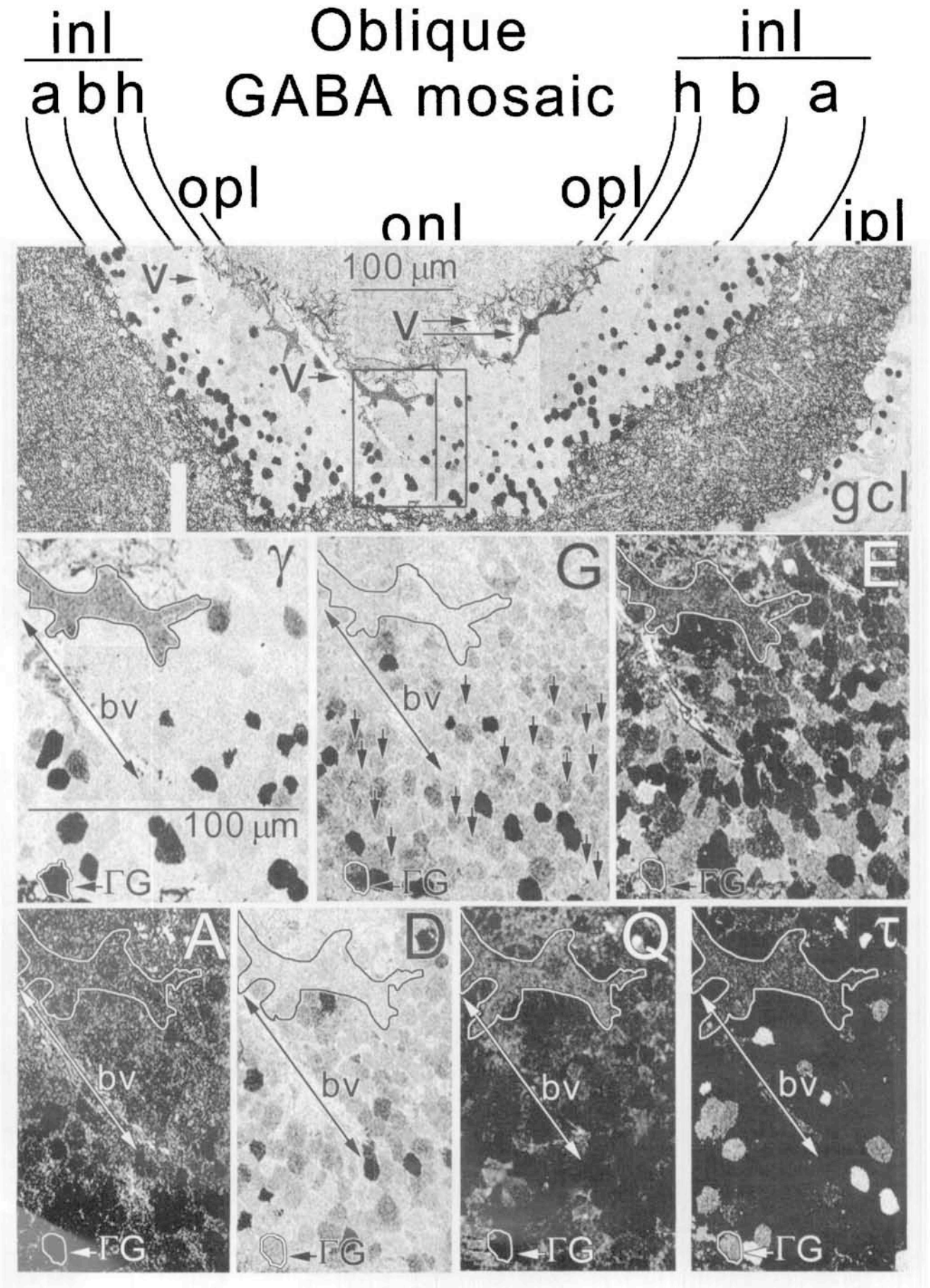
inl
a b h
Oblique
GABA mosaic
inl
h b a
opl
opl
onl
ipl
100 µm
V
V
V
gcl
γ
bv
100 µm
ГG
G
bv
ГG
E
ГG
A
bv
ГG
D
bv
ГG
Q
bv
ГG
τ
bv
ГG

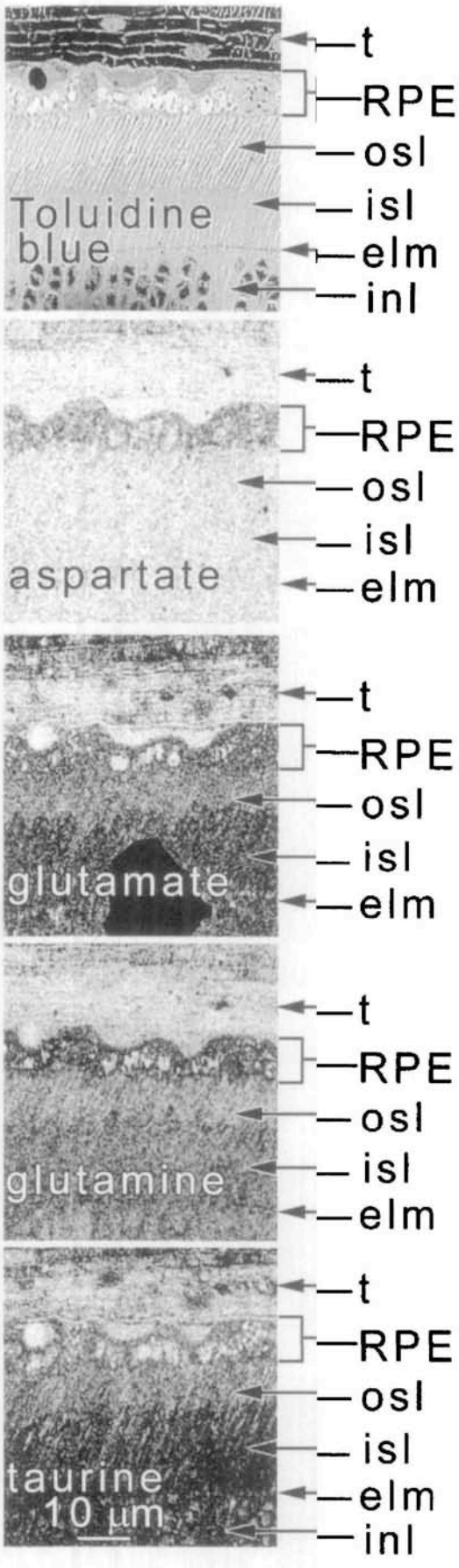

cells, but augmented by moderate levels of glutamate and aspartate.

Discussion

Origins and Significances of Signatures

Any intracellular amino acid level assayed by immunocytochemistry represents the balance between amino acid sources and sinks. The sources of amino acids for any cell are synthesis of nonessential amino acids at rates determined by the activities of specific enzymes, selective transport from the extracellular space, and adventitious diffusional leakage through heterologous gap junctions. Sinks are more complex and include varied enzymatic conversions, assimilation into proteins, vesicular synaptic release, reverse transport and adventitious leakage through gap junctions. The strong similarities in patterns of amino acid signatures across species suggest that most cell-specific signatures represent a characteristic dynamic equilibrium in all sources and sinks.[4,5,12] For example, γ^{+} horizontal cells in fishes, avians, cats, and primates share a similar signature whose GABA signal is lower than that of any amacrine cell. Because the key divergence between osteichthyan fishes and tetrapods occurred 400 million years ago, horizontal cell signatures seem to reflect a strongly conserved biochemistry. Certain major signature types correlate with inferred function: Class **E** cells as glutamatergic, class **G** as glycinergic, and class Γ as GABAergic. However, because all cells may contain some glutamate and glycine as precursors, there is no absolute amino acid level that unambiguously defines glutamatergic or glycinergic cells in all instances. Close examination of the signature matrix (Fig. 4) formally proves that glutamate content alone is an insufficient index of glutamatergic function, in that most neurons have substantial glutamate contents with distributions that overlap into the ranges shown by photoreceptors, bipolar cells, and ganglion cells. As in all other vertebrates thus far examined, multiple amino acid signals are required to group neurons into putative glutamatergic, GABAergic, or glycinergic classes on a quantitative basis.

Conventional Neuronal and Glial Signatures in Retinal Space

As revealed in Figure 1 and documented in previous studies,[4,5,12] essentially all cells in all layers possessed a distinctive signature that parsed them into glial, class **E** neuronal, class **G** neuronal, class Γ neuronal, or RPE compartments. The largest fields of unclassified space were the lumens of blood vessels. Further, the only cell layer in which we occasionally encountered clearly unclassifiable cells was the amacrine cell layer, similar to findings by Kalloniatis et al.,[5] and far less than 1% of cells in the amacrine cell layer had no definable amino acid signature. This could be because of the existence of bona fide

FIGURE 3. Serial, registered 200-nm sections displaying amino acid signals in the retinal pigment epithelium (RPE). *Top*: a toluidine blue–stained section. The RPE possessed distinctive amino acid signals that were greater than (aspartate, glutamine) or closely matched to (glutamate, taurine) those of photoreceptor cells. The tapetum (t) contained very low free amino acid signals.

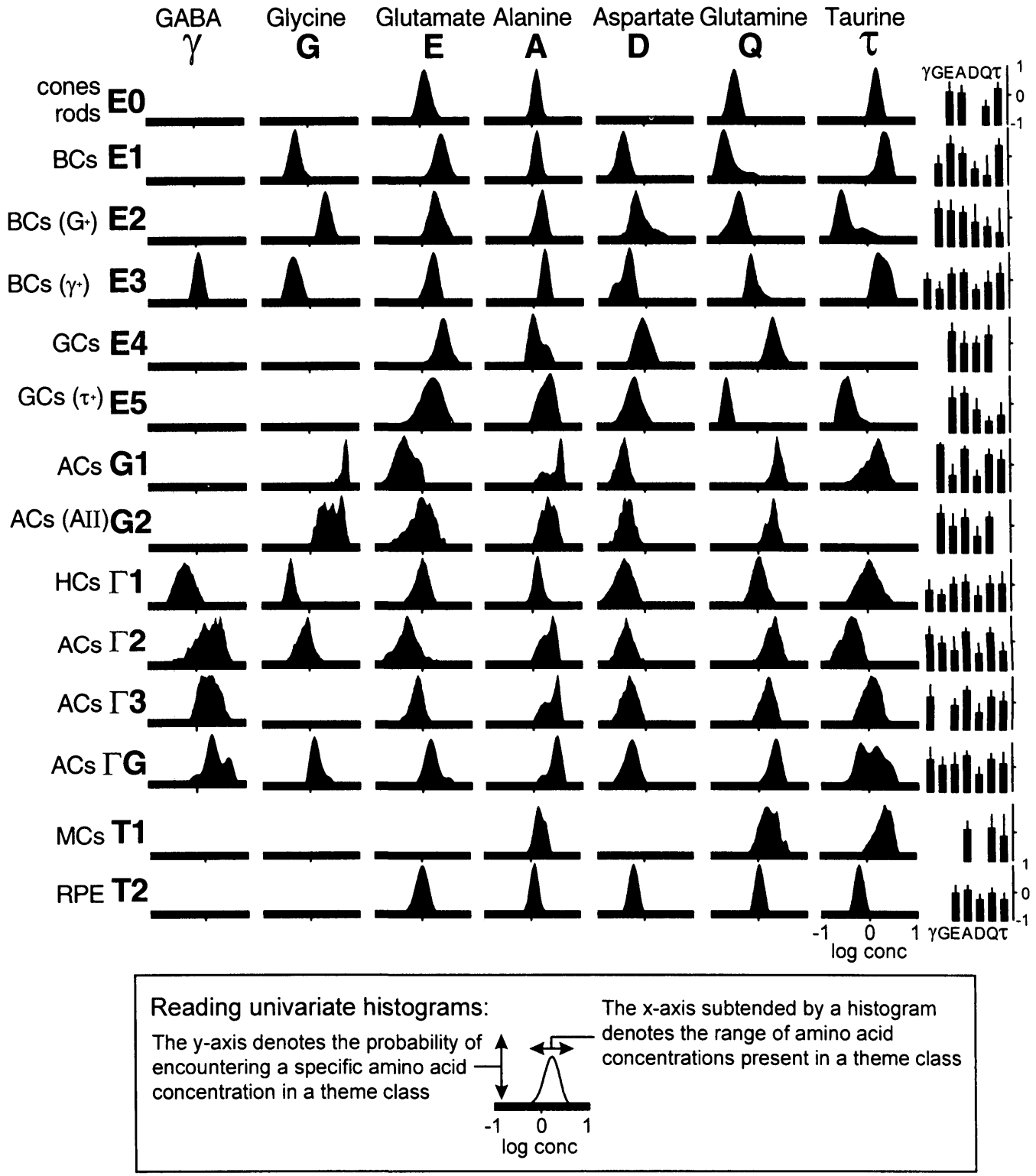

Figure 4. The signature matrix for the normal cat retina. The *left column* identifies corresponding cell and theme classes. Amino acids are grouped in *vertical columns*: γ, GABA; G, glycine; E, glutamate; A, alanine; D, aspartate; Q, glutamine; and τ, taurine. Each column shows the distribution of a single amino acid across all theme classes, and each row is the univariate signature for each class. All probability density distributions are amplitude normalized; the *y*-axis denotes the relative probability of encountering a given amino acid level along an *x*-axis of increasing log amino acid concentration. Histograms were fast-Fourier transform-filtered to yield a resolution of approximately 16 Hz, that is, 16 unique concentration levels in 0.125 log unit steps in discrete terms. Signals with roughly −1 log unit mean concentration are not included because they approach the limits of quantitative resolution for immunocytochemistry. The *right column* for each row is a bar graph of all seven modal amino acid values for each cell class and an error bar equivalent to ±3 SD for a single gaussian. The height of each bar is scaled logarithmically.

neurons that normally have no glutamate, GABA, or glycine; the presence of nonneuronal elements in the amacrine cell layer with no definable signature; and incidental necrotic cell death or trauma in the "normal" retina incurred during fixation. We have no resolution on this point except to note that small patches of apparently traumatized cells occur in otherwise well-perfused or immersion-fixed material from many species. It is also certain that microglia, which are widely distributed in mammalian retinas,[18,19] remain unclassified or are merged with another signature class. It is possible that the microglial signature and small somatic size predispose them to be statistically inseparable with our current spectrum of amino acid probes.

Subdividing the Signatures of Fundamental Retinal Cell Types

Cat rods and cones had a similar type **E0** signature that was different from other putative glutamatergic cells in having a very low aspartate content and a moderate (roughly 1 mM) glutamate signal. This again emphasizes that glutamate content alone is an insufficient marker of glutamatergic function and that bona fide glutamatergic cells can operate with low levels of endogenous glutamate.[4] Bipolar cells are divisible into relatively glycine-poor (**E1, E3**) and glycine-rich (**E2**) varieties. The former probably represent a mixture of ON center rod bipolar cells (**E1**) and OFF center cone bipolar cells (**E1** and **E3**). **E2** cells represent the ON center cone bipolar cell cohort whose glycine content is probably derived by diffusion through gap junctions they form with glycinergic amacrine cells.[20] This model is supported by recent studies showing that all bipolar cells in rabbit retina (including rabbit **E2** bipolar cells) do not have the GLYT1 high-affinity glycine transporter[21]; a high glycine content in bipolar cells is thus unlikely to arise from direct high-affinity glycine uptake. Although amacrine cell glycine signals tend to be stable across preparations, the glycine signal in mammalian **E2** bipolar cells is extremely variable (Marc RE, unpublished data, 1993-1998), consistent with their glycine content arising partially from variable adventitious sources. Cat bipolar cells equivalent to primate class **E3** bipolar cells[5] containing weak γ^+ signals have been described previously by Wässle and Chun[22] and Vardi and Shi.[23] They are rare cells compared with **E1** and **E2** bipolar cells, and their function is unknown.

Ganglion cell signatures in cat closely resemble those of the primate retina[5] for types **E4** and **E5**, but cat retina apparently has no distinctive population of γ^+ ganglion cells that can be found at low densities in the macaque[5] and relatively high numbers in rabbit.[24,25] Notably, γ^+ ganglion cells are altogether absent in teleost fish retinas. Given the massive divergences among these models, the presence or absence of γ^+ ganglion cells must be considered an apomorphism.

The simplest but perhaps most relevant part of this analysis is the demonstration of a characteristic **T1** signature for Müller cells expressing minimal glutamate signals. Müller cells in all known species show robust glutamate transport[26,27] and are also the sole retinal cells known to express the enzyme glutamine synthetase,[28,29] which is essential for recycling carbon skeletons. The signature of normal Müller cells thus reflects the following normal dynamic equilibrium: Glutamate released by retinal neurons and transported into Müller cells is partially buffered by glutamine synthetase activity to extremely low intracellular levels, with concomitant accumulation of glutamine. Lewis et al.[30] have shown that experimental retinal detachment leads to a range of disturbances in the expressions of macromolecules in Müller cells, including a significant decrease in glutamine synthetase immunoreactivity beginning as early as 2 days after detachment.[31] Thus, concomitant disruptions in primary micromolecular signatures can be expected to occur in Müller cells after retinal detachment. Müller cells also have robust GABA transport,[26] yet show no measurable basal GABA signal, consistent with their known content of GABA transaminase as the primary mechanism of GABA turnover.[32,33]

Although the RPE is not normally considered part of glutamatergic or GABAergic neurochemical cycles, mammalian RPE cells possess GABA[34] transporters and glutamate[35] transport. The absence of any GABA signal in the RPE implies that no significant GABA concentrations normally develop in the subretinal space or that RPE cells have a very high GABA turnover rate. There is no evidence for the latter. The RPE shows a basal signature with elevated glutamate, aspartate, and glutamine signals. Whether RPE cells generate these signals through endogenous synthetic paths or transport is unknown.

The micromolecular content of any cell is linked to intracellular sources and sinks closely associated with the intracellular respiratory state and extracellular sources and sinks dependent on complex factors such as physical proximity of cell compartments, blood flow, and the integrity of various transporting cells or cells responsible for key metabolic conversions. Thus disruptions in any of these processes, whether arising from trauma or inherited disease, are expected to be reflected in altered micromolecular signatures in general and amino acid signatures in particular. Such alterations may be detectable and perhaps even interpretable, because different insults should affect different pathways and evoke differential patterns of amino acid content. This has already proved true: Fletcher and Kalloniatis[36,37] have shown clear anomalies in Müller cell glutamate metabolism in the RCS rat retina, implying that the lesion is multifactorial and involves an array of defects that appear most graphically as photoreceptor degeneration.

References

1. Kolb H, Nelson R, Mariani A. Amacrine cells, bipolar cells and ganglion cells of the cat retina. *Vision Res.* 1981;21:1081-1114.
2. Schnitzer J. Astrocytes in mammalian retina. *Prog Retinal Res.* 1988;7:209-232.
3. Holländer H, Makarov F, Dreher Z, van Driel D, Chan-Ling T, Stone J. Structure of the macroglia of the retina: sharing and division of labour between astrocytes and Müller cells. *J Comp Neurol.* 1991; 313:587-603.
4. Marc RE, Murry RF, Basinger SF. Pattern recognition of amino acid signatures in retinal neurons. *J Neurosci.* 1995;15:5106-5129.
5. Kalloniatis M, Marc RE, Murry RF. Amino acid signatures in the primate retina. *J Neurosci.* 1996;16:6807-6829.
6. Kolb H, Nelson R. The organization of photoreceptor to bipolar synapses in the outer plexiform layer. In: Djamgoz MBA, Archer SN, Vallerga S, eds. *Neurobiology and Clinical Aspects of the Outer Retina.* London: Chapman & Hall; 1995:274-324.
7. Fisher SK, Erickson PA, Lewis GP, Anderson DH. Intraretinal proliferation induced by retinal detachment. *Invest Ophthalmol Vis Sci.* 1991;32:1739-1748.
8. Leonard DS, Zhang X-G, Panozzo G, Sugino IK, Zarbin M. Clinicopathologic correlation of localized retinal pigment epithelium débridement. *Invest Ophthalmol Vis Sci.* 1997;38:1094-1109.
9. Stone J, Maslim J. Mechanisms of retinal angiogenesis. *Prog Retinal Eye Res.* 1997;16:157-181.

10. Duffy TE, Nelson SR, Lowry OH. Cerebral carbohydrate metabolism during acute hypoxia and recovery. *J Neurochem.* 1972;19: 959-977.
11. Plaitakis A, Berl S, Yahr MD. Abnormal glutamate metabolism in an adult-onset degenerative neurological disorder. *Science.* 1982;216: 193-196.
12. Kalloniatis M, Tomisich G, Marc RE. Neurochemical signatures revealed by glutamine labeling in the chicken retina. *Vis Neurosci.* 1994;11:793-804.
13. Marc RE, Liu W-LS, Kalloniatis M, Raiguel S, Van Haesendonck E. Patterns of glutamate immunoreactivity in the goldfish retina. *J Neurosci.* 1990;10:4006-4034.
14. Kalloniatis M, Fletcher E. Immunocytochemical localization of the amino acid neurotransmitters in the chicken retina. *J Comp Neurol.* 1993;336:174-193.
15. Swain PH, Davis SM. *Remote Sensing: A Quantitative Approach.* New York: McGraw-Hill; 1978.
16. Yazulla S, Yang C-Y. Colocalization of GABA and glycine immunoreactivities in a subset of retinal neurons in the tiger salamander. *Neurosci Lett.* 1988;95:37-41.
17. Kalloniatis M, Tomisch G. Glycine and GABA in amacrine cells of the cat retina [ARVO Abstract]. *Invest Ophthalmol Vis Sci.* 1995; 36(4):S286. Abstract nr 1330.
18. Boycott BB, Hopkins JM. Microglia in the retina of monkey and other mammals: its distinction from other type of glia and horizontal cells. *Neuroscience.* 1981;6:679-688.
19. Schnitzer J. Enzyme-histochemical demonstration of microglial cells in the adult and postnatal rabbit retina. *J Comp Neurol.* 1989;282:249-263.
20. Cohen E, Sterling P. Accumulation of (^{3}H) glycine by cone bipolar neurons in the cat retina. *J Comp Neurol.* 1986;250:1-7.
21. Koomen JM, Lehr KP, Massey SC. The glycine transporter, GlyT1, is localized to AII amacrine cells but not coupled cone bipolar cells in the rabbit retina [ARVO Abstract]. *Invest Ophthalmol Vis Sci.* 1997;38(4):S47. Abstract nr 222.
22. Wässle H, Chun MH. GABA-like immunoreactivity in the cat retina: light microscopy. *J Comp Neurol.* 1989;279:43-54.
23. Vardi N, Shi J-Y. Identification of GABA containing bipolar cells in cat retina [ARVO Abstract]. *Invest Ophthalmol Vis Sci.* 1996; 37(3):S418. Abstract nr 1938.
24. Yu BC-Y, Watt CB, Lam DMK, Fry KR. GABAergic ganglion cells in the rabbit retina. *Brain Res.* 1988;439:376-382.
25. Marc RE. Neurochemical and glutamatergic response signatures in the retinal ganglion cell layer [ARVO Abstract]. *Invest Ophthalmol Vis Sci.* 1997;34(4):S689. Abstract nr 3214.
26. Ehinger B, Falck B. Autoradiography of some suspected neurotransmitter substances: GABA, glycine, glutamic acid, aspartic acid, histamine, dopamine and [l]-dopa. *Brain Res.* 1971;33:157-172.
27. Brew H, Attwell D. Electrogenic glutamate uptake is a major current carrier in the membrane of axolotl retinal glial cells. *Nature.* 1987;327:707-709.
28. Riepe RE, Norenburg MD. Müller cell localisation of glutamine synthetase in rat retina. *Nature.* 1977;268:654-655.
29. Moscona AA. On glutamine synthetase, carbonic anhydrase and Müller glia in the retina. *Prog Retinal Res.* 1983:2;111-135.
30. Lewis, GP, Erickson PA, Guèrin CJ, Anderson DH, Fisher SK. Changes in the expression of specific Müller cell proteins during long-term retinal detachment. *Exp Eye Res.* 1989;49:93-111.
31. Lewis, GP, Erickson PA, Guèrin CJ, Anderson DH, Matsumoto B, Fisher SK. Rapid changes in the expression of glial cell proteins caused by experimental retinal detachment. *Am J Ophthalmol.* 1994;118:368-376.
32. Robin LM, Kalloniatis M. Interrelationship between retinal ischemic damage and turnover and metabolism of putative amino acid neurotransmitters, glutamate and GABA. *Doc Ophthalmol.* 1992;1992:30:273-300.
33. Neal MJ, Cunningham JR, Shah MA, Yazulla S. Immunocytochemical evidence that vigabatrin in rats causes GABA accumulation in glial cells of the retina. *Neurosci Lett.* 1989;98:29-32.
34. Johnson J, Chen TK, Rickman DW, Evans C, Brecha N. Multiple γ-aminobutyric acid plasma membrane transporters (GAT-1, GAT-2, GAT-3) in the rat retina. *J Comp Neurol.* 1996;375:212-224.
35. Miyamoto Y, Del Monte MA. Na^+-Dependent glutamate transporter in human retinal pigment epithelial cells. *Invest Ophthalmol Vis Sci.* 1994;35:3589-3598.
36. Fletcher EL, Kalloniatis M. Neurochemical architecture of the normal and degenerating rat retina. *J Comp Neurol.* 1996;376:343-360.
37. Fletcher EL, Kalloniatis M. Localization of amino acid neurotransmitters during postnatal development of the rat retina. *J Comp Neurol.* 1997;380:449-471.